

# Viscosity of Foaming Fluid Measured by Falling-Ball Method

*S Ueda*<sup>1</sup>, *T Iwama*<sup>2</sup> *Y Mita*<sup>3</sup> and *R Inoue*<sup>4</sup>

<sup>1</sup> Professor, Tohoku University, Sendai Miyagi 980-8577. tie@tohoku.ac.jp

<sup>2</sup> Assistant Professor, Tohoku University, Sendai Miyagi 980-8577.  
takayuki.iwama.a6@tohoku.ac.jp

<sup>3</sup> Graduate student, Tohoku University, Sendai Miyagi 980-8577.  
yusaku.mita.p1@alumni.tohoku.ac.jp

<sup>4</sup> Researcher, Tohoku University, Sendai Miyagi 980-8577. ryo.inoue.e2@tohoku.ac.jp

Keywords: foaming slag, apparent viscosity, EAF slag, multiphase fluid

## ABSTRACT

In the iron and steel manufacturing industries, efforts are being made to achieve carbon neutrality by 2050, and the transition from a coal-based steelmaking process to that utilizing renewable energy is being pursued. An alternative process in which directly hydrogen-reduced iron is melted in an electric furnace is being investigated. It is known that foaming slag reduces heat loss from the steel bath in electric arc furnace, but iron loss due to the suspension of steel particles in the slag is indispensable. To improve the separation of steel particles from the slag, the control of the slag viscosity is important.

Although the slag viscosity has been extensively studied, in those studies the slag was considered to be a simple liquid. However, in actual operations, slag is a multiphase fluid consisting of solid, gas, and liquid phases. Therefore, in this study, by measuring the sedimentation velocity of titanium, stainless steel and glass spheres in an aqueous glycerin solution containing bubbles generated by the reaction between  $\text{NaHCO}_3$  and  $\text{C}_2\text{H}_2\text{O}_4$ , the apparent viscosity of the gas-liquid fluid was evaluated based on Stoke's law. It was found that the apparent viscosity of the gas-liquid fluid is larger than the viscosity of liquid phase and depends on both the bubble volume ratio in solution and the density of the falling solid sphere, and the apparent viscosity was different from that previously obtained by the rotation method. The apparent viscosity derived from the sedimentation velocity of solid spheres changed depending on the specific gravity of the ball. This is because the apparent viscosity is derived from the velocity of a ball falling in a static bubble in this method, whereas that is derived from the force applied by a stationary flow in the rotational method.

## INTRODUCTION

Currently, carbon neutrality in steel production is required to combat global warming. Since the conventional blast furnace/converter process mainly uses coke as a reductant, even when some of the coke is replaced with hydrogen-based reductants,  $\text{CO}_2$  reductions are limited. On the other hand, the electric arc furnace (EAF) steelmaking method, which usually uses scrap as raw material, requires less energy for steel production, resulting in lower  $\text{CO}_2$  emissions. For this reason, it is predicted that the proportion of steel produced by electric furnace could increase in the future.

When EAF steelmaking becomes the mainstream, steel scrap is smelted repeatedly, causing a cycle of elements contained in the scrap. In particular, the concentration of elements called tramp elements such as Cu and Sn, which cannot be removed by oxidation refining, is a serious concern. To control the concentration of such circulating elements, it is necessary to use pig iron and reduced iron sources. Direct Reduced Iron (DRI), reduced by hydrogen, etc., is expected to be a raw material free of circulating elements. However, DRI contains gangue components (oxides), which are the source of slag. Therefore, more slag is produced in DRI melting than conventional scrap melting.

At the end of the EAF smelting process, the slag is foamed by CO gas generated by the coal material blown into the furnace. This foaming slag functions as a heat insulator for molten steel, improving

heat transfer efficiency from the arc and contributing to reducing CO<sub>2</sub> emissions. On the other hand, iron particles are easily entrapped in the foaming slag phase. When those particles do not fall down and remain in the slag, it causes iron loss, i.e., lower iron yield. Although iron particles fall into the slag after long static holding, which improves the iron yield, it must be balanced against the productivity of the process. Since slag viscosity is an important property in predicting the sedimentation velocity of iron particles, it has been measured for many slag systems. However, most measurements were performed on single-phase liquids.

For solid-gas-liquid multiphase fluids such as EAF slag, the viscosities reported for single slag melts are not applicable. The properties of slag-based multiphase fluids had been measured within limited experimental conditions. Saito et al.(2020) measured the viscosity of silicone oil, in which polyethylene beads were suspended, by a fluid-rotation method. They derived an empirical formula based on the following Einstein-Roscoe's equation proposed by Roscoe (1952).

$$\frac{\eta_{SL}}{\eta_L} = (1 - \phi_s)^{-2.5} \quad (1)$$

where  $\eta_{SL}$  [mPa·s]: viscosity of solid-liquid fluid,  $\eta_L$ [mPa·s]: viscosity of liquid phase, and  $\phi_s$ : volume fraction of dispersed solid phase in solid-liquid fluid.

Li et al. (2022) also measured the viscosity of the same mixture by a falling-ball method. However, the viscosity obtained was lower than that measured by the rotational method. In their study, the mixture exhibited dilatant fluid behaviour with properties different from those obtained by the rotational method.

The viscosity of gas-liquid fluids simulating foaming slag has been studied only by Martinsson (2018) and Hatano et al.(2021). Hereafter, this viscosity is called 'apparent viscosity' to distinguish it from that of a single liquid. In the present study, the apparent viscosity of gas-liquid fluid was measured by the falling-ball method based on Stokes' equation to confirm the difference from that obtained by the rotation method. For the evaluation of the sedimentation velocity of iron particle in the gas-liquid fluid, it is necessary to consider not only the macroscopic viewpoint of the sedimentation velocity of dispersed particles in the foaming fluid but also the microscopic viewpoint of the morphology of foams around the particle, so the sedimentation behaviour of solid particle was observed simultaneously with the measurement of apparent viscosity.

## EXPERIMENT

### Sample preparation

To create a gas-liquid fluid simulating foaming slag at room temperature, the method proposed by Saito et al.(2020), in which CO<sub>2</sub> gas is generated by mixing and reacting a C<sub>2</sub>H<sub>2</sub>O<sub>4</sub>-saturated aqueous solution with a glycerine aqueous solution containing NaHCO<sub>3</sub>, was employed. The glycerin concentrations  $X_{\text{Glycerin}}$  in weight fraction after mixing were 0.20, 0.35, 0.50, 0.65, and 0.80, whose viscosities  $\eta_L$  are 1.76, 3.06, 6.01, 15.2, and 60.1 mPa·s, respectively. To increase the generation rate and stability of bubbles, 0.1 g of polyoxyethylene-laurylether, a surfactant, was added to the NaHCO<sub>3</sub> solution.

In the viscosity measurements, three types of spheres with different densities were used as sedimentation particles: stainless steel sphere (density  $\rho_p = 7.93 \text{ g/cm}^3$ ), titanium sphere ( $\rho_p = 4.51 \text{ g/cm}^3$ ), and glass beads ( $\rho_p = 2.50 \text{ g/cm}^3$ ). The diameter of these spheres was chosen to be 2.0 mm because it is close to the maximum size of iron particles observed in the slag and easy to observe during measurement. These particles were pre-wetted with glycerin solution to smooth the initial sedimentation.

### Experimental apparatus

Figure 1 presents an overview of the experimental setup. The bath is a rectangular made of acrylic plate with a thickness of 3 mm, whose internal dimensions are 25 mm × 44 mm in horizontal cross section (cross-sectional area  $A=0.0011 \text{ m}^2$ ) and 326 mm in height. By installing a glass filter (6 mm thickness, open pore size = 100-120  $\mu\text{m}$ ) at a height of 20 mm from the inner bottom of the bath, it is possible to separate the  $\text{NaHCO}_3$ -glycerine solution above the filter from the  $\text{C}_2\text{H}_2\text{O}_4$  solution injected from the bottom.

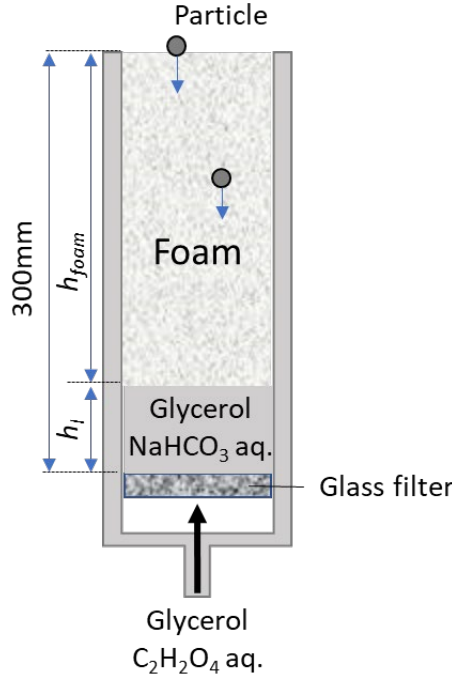


FIG 1 Experimental apparatus of the falling-ball method for creating gas-liquid fluid.

## Experimental procedure

In this study, the gas-phase volume fraction  $\phi_g$  of the obtained gas-liquid fluid is defined as follows.

$$\phi_g = \frac{h_0 - h_L}{h_0} \left( = \frac{h_{foam}}{h_0} \right) \quad (2)$$

where  $h_0$  [m]: maximum height of gas-liquid fluid (0.30 m),  $h_L$  [m]: height in single liquid phase,  $h_{foam}$  [m]: height in gas-liquid phase. Gas-liquid fluids with  $\phi_g=0.5$  and 0.7 were created by adjusting the  $\text{NaHCO}_3$  concentration and mixing ratio of two solutions. The total amount of  $\text{NaHCO}_3$  solution and  $\text{C}_2\text{H}_2\text{O}_4$  solution charged in the apparatus was determined to fill the volume above the glass filter, which is  $A \times h_0$  [ $\text{m}^3$ ], with the gas-liquid fluid. When these two solutions are mixed, the volume of the liquid phase without foaming is  $A \times h_0 \times (1 - \phi_g)$  [ $\text{m}^3$ ]. On top of the generated gas-liquid fluid, several stainless steel, titanium, and glass spheres were gently placed. The falling behaviour of these particles was photographed continuously with a video camera. The sedimentation velocity of the spheres was derived from the video image by measuring the transit time every 5 mm in a 150 mm section from the bath depth of 50 mm to 200 mm while watching.

## Derivation of apparent viscosity of gas-liquid fluids

In the falling-ball method, the viscosity of a single liquid  $\eta_L$  can be derived from the sedimentation velocity of a sphere using the following Stokes equation.

$$\eta_L = \frac{D_P^2(\rho_P - \rho_L)}{18U}g \quad (3)$$

where  $D_P$  [m]: diameter of a sedimentation particle,  $\rho_P$  [kg/m<sup>3</sup>]: density of a sedimentation particle,  $\rho_L$  [kg/m<sup>3</sup>]: density of a fluid,  $U$  [m/s]: sedimentation velocity of a particle, and  $g$  [m/s<sup>2</sup>]: gravitational acceleration. Although this equation (3) is applicable only to Newtonian fluids, it is assumed that the equation can be applied to a gas-liquid fluid in the analysis of this study.

When the density of a gas-liquid fluid can be expressed as  $(1 - \phi_g)\rho_L$ , the apparent viscosity of gas-liquid fluid  $\eta$  derived from equations (2) and (3) will be as follows.

$$\eta = \frac{D_P^2(\rho_P - (1 - \phi_g)\rho_L)}{18U}g \quad (4)$$

## RESULTS AND DISCUSSION

The apparent viscosity of gas-liquid fluid at  $\phi_g=0.7$  was measured by the falling-ball method while changing the viscosity of liquid, which composes foams.

Figure 2a shows the relationship between the elapsed time and the position of stainless steel and titanium spheres sedimented in the foaming glycerin solution with  $\eta_L=60.1$  mPa·s.

The experimental points marked ● and ◆ in this figure represent the results for stainless steel sphere and titanium sphere, respectively. The different colors of the symbols indicate the different trajectories of stainless steel and Ti spheres. It can be seen that in the gas-liquid fluid under this condition, both the stainless steel and titanium spheres descend while pushing away the bubbles, and that the sedimentation velocity of stainless steel spheres with high density is higher than that of titanium spheres with low density.

The apparent viscosity  $\eta$  derived from the sedimentation velocity of stainless steel and titanium spheres using equation (4) is 419 and 671 mPa·s, respectively. The latter is particularly large. These values are large compared to the viscosity of single liquid phase,  $\eta_L = 60.1$  mPa·s. The apparent viscosity could not be determined from the sedimentation velocity of the glass beads because they were trapped between bubbles and did not sediment.

Figure 2b shows a binarized image of a gas-liquid fluid with  $\phi_g=0.7$  immediately after foaming. Large bubbles with diameters of 1.0 to 1.5 mm are found to be homogeneously distributed. Since it is expected that in this glycerine aqueous solution, the high viscosity of liquid decreases the liquid drainage rate in the bubble film, slowing down the generation of bubbles, it took about 2 minutes to reach the desired gas phase fraction. Meanwhile, the bubbles have grown.

Figure 3a shows the time dependence of the falling length of stainless steel, titanium, and glass spheres in a gas-liquid fluid of glycerine solution with  $\eta_L=6.01$  mPa·s. The spheres made of stainless steel, titanium, and glass all descended, pushing away the bubbles and reaching the terminal velocity. The apparent viscosity  $\eta$  derived from the terminal velocity of each sphere was 340, 415, and 439 mPa·s, respectively. Although these values were larger than that of the liquid phase, there were no significant differences depending on the type of falling sphere. As shown in Figure 3b, foams were generated quickly, and the packing of fine bubbles was maintained until the drainage in the liquid film progressed. No bubbles with a diameter larger than 1 mm were observed during this period.

The sedimentation of stainless steel and titanium spheres in a gas-liquid fluid in a glycerin solution with  $\eta_L=1.76$  mPa·s is shown in Figure 4a. As is seen in Figure 4b, the foams are not homogeneous in size, and the forming region is divided into two parts: a region with coarsened bubbles in the upper part, and that with dense bubbles in the lower part. The stainless steel spheres descended while breaking the coarsened bubbles, and its terminal velocity was reached at 0.6 sec after falling. In the case of the titanium sphere, the sedimentation velocity is slow in the upper region and increases in

the lower region. The titanium sphere did not break the bubbles and was repeatedly accelerated and decelerated due to the movement by pushing the bubbles away and stopping by the bubbles. The glass sphere was suspended at the top of the fluid and did not fall down. Therefore, it was considered difficult to derive the apparent viscosity of the gas-liquid fluid from the sedimentation velocity of the titanium spheres and glass beads. From the terminal velocity of the stainless steel spheres,  $\eta=50$  mPa·s was derived, approximately 28 times larger than the viscosity of the single liquid phase.

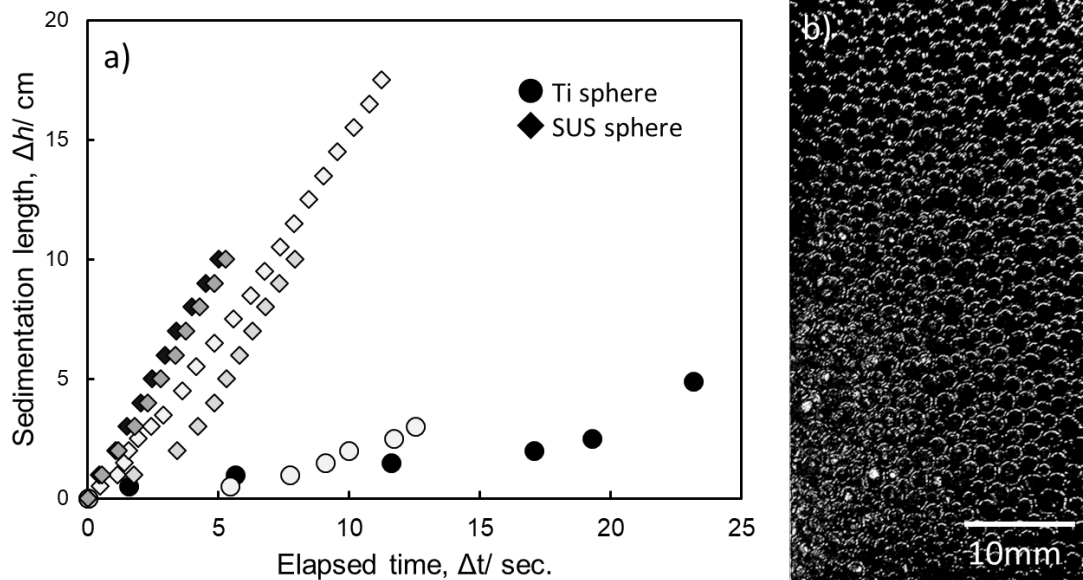


FIG 2 Particle descent behavior (a) and foam morphology (b) in glycerin solution with  $\eta_L=60.1$  mPa·s.

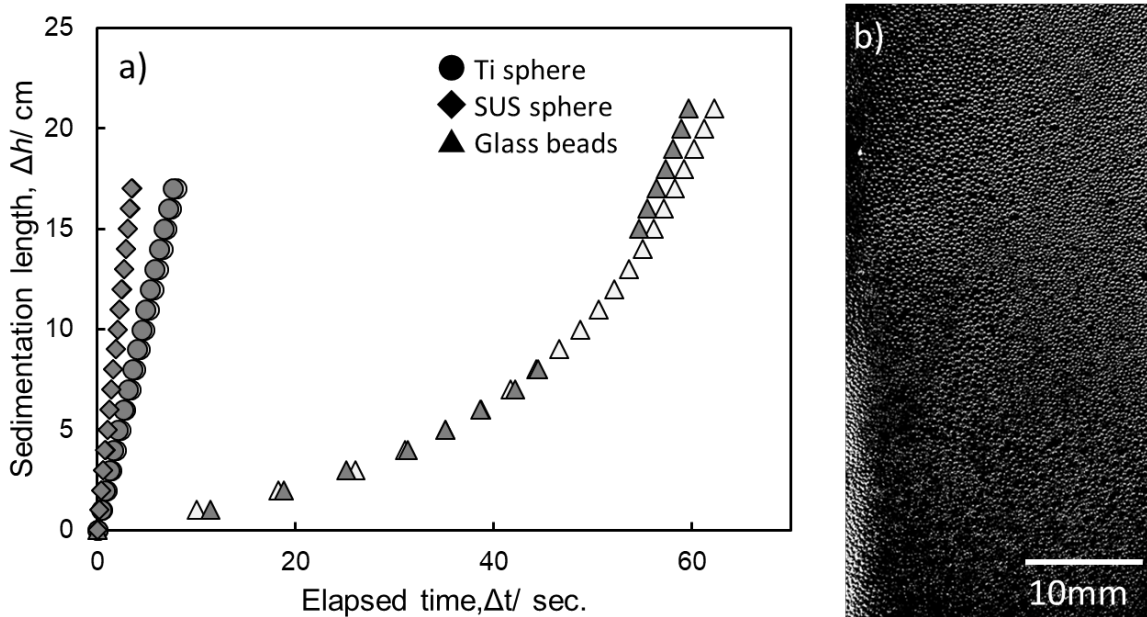


FIG 3 Particle descent behavior (a) and foam morphology (b) in glycerin solution with  $\eta_L=6.01$  mPa·s.

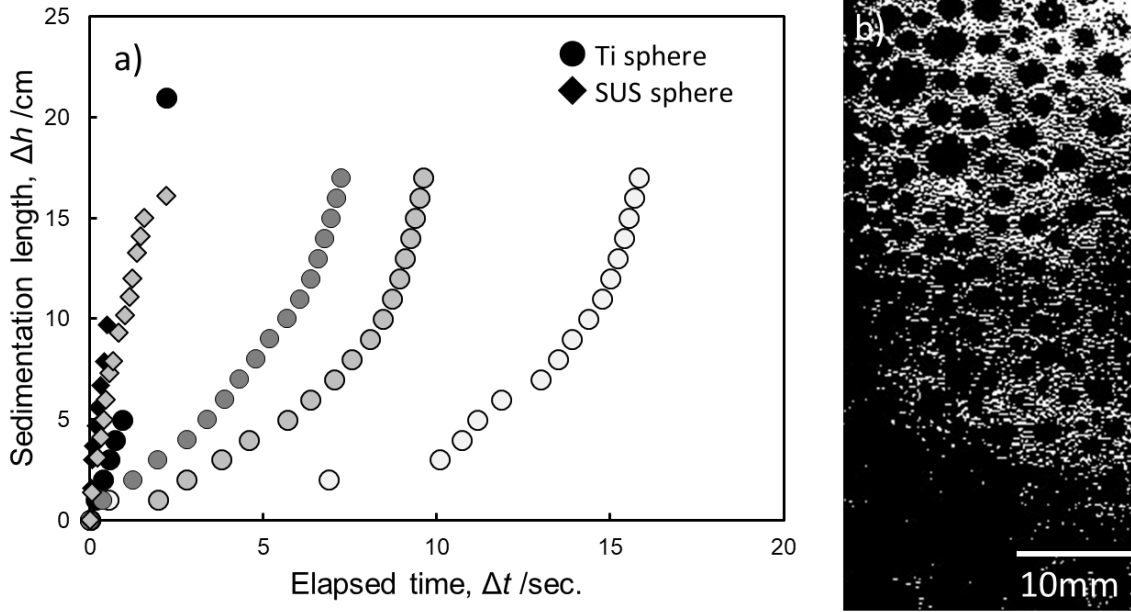


FIG 4 Particle descent behavior (a) and foam morphology (b) in glycerin solution with  $\eta_L=1.76$  mPa·s.

## RELATIONSHIP BETWEEN LIQUID VISCOSITY AND APPARENT VISCOSITY OF FOAM

The apparent viscosities of the gas-glycerin solution systems at  $\phi_g=0.7$  obtained in this study are compared with those determined by Hatano et al.(2021) using the rotational method.

Figure 5 shows the relationship between the viscosity of liquid-phase and the apparent viscosity of the foaming gas-liquid fluid. The apparent viscosity measured by the falling-ball method using stainless steel and Ti balls is shown by a solid line and a broken line, respectively, and that measured by Hatano et al.(2021) using the rotation method at 50 and 100 r.p.m. is shown by a gray dotted line and a gray dash-dotted line, respectively. Regardless of the measurement method, the apparent viscosity shows an increasing behaviour as a logarithmic function of the viscosity of single liquid phase. In the falling-ball method, the apparent viscosity estimated using stainless steel spheres is lower than that using titanium spheres because the sedimentation velocity  $U$  in equation (4) of the stainless steel sphere is higher. The apparent viscosity measured by the rotation method tends to decrease with increasing rotational velocity. Therefore, it can be concluded that both measurement methods show similar results regarding the decrease in apparent viscosity with an increase in the velocity of the moving object. Under the present experimental condition, the apparent viscosities derived from the sedimentation velocity of stainless steel and titanium spheres with a diameter of 2 mm are in good agreement with those obtained at rotational velocity of 50 and 100 r.p.m. in rotation method, respectively.

The falling-ball method utilizes particle sedimentation, and the rotation method uses constant rotation of a cylinder. Since the motion of the moving object is different in those two methods, it is not necessary that the values for apparent viscosity obtained by each method be equal to each other. However, it was found in this study that the apparent viscosity of gas-liquid fluid obtained by falling-ball method is comparable to that by the rotation method. Further accumulation of experimental data in the future may lead to derive a quantitative relationship between rotation rate and sedimentation velocity.

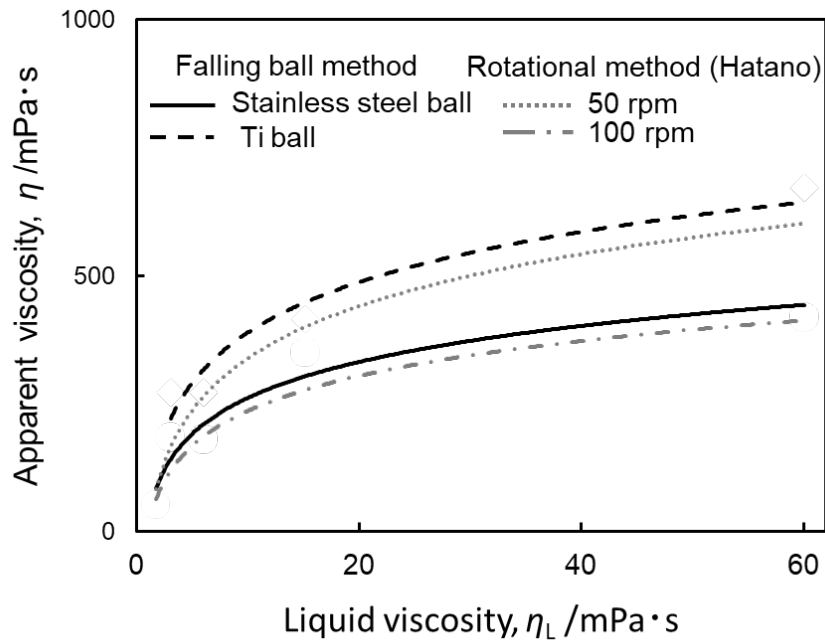


FIG 5 Comparison of apparent viscosity of gas-liquid fluid estimated by the falling-ball method and rotation method.

## CONCLUSIONS

To understand the sedimentation behaviour of iron particles suspended in foaming slag, the apparent viscosity of a gas-liquid fluid with glycerin solution was estimated by the falling-ball method.

The apparent viscosity obtained was larger than the viscosity of a single liquid phase. When the viscosity of the liquid phase is large, the particles fall while pushing away the bubbles and sewing the liquid part of the foam film since the progress of liquid drainage is slow and wet foam can be easily maintained. However, under the present experimental condition, particles with low density, such as glass beads, could not push bubbles away and did not fall. The higher the density of particles, the smaller the apparent viscosity of the gas-liquid fluid derived by the Stokes law.

## REFERENCES

- Glycerine Producer's Association, 1969. Physical Properties of Glycerine and Its Solutions., New York
- Hatano, S, Hayashi, S, Saito, N, Nakashima, K, 2021. Viscosity Evaluation of Simulated Foaming Slag via Interfacial Reaction at Room Temperature, *ISIJ Int.*, 61:2904–2914.
- Li, W, Iwama, T, Yu, H, Ueda, S, Saito, N, Inoue, R, 2021. Apparent Viscosity Measurement of Solid-liquid Coexisting Fluid by Falling Ball Method for Evaluation Iron Particle Sedimentation Velocity in Slag, *ISIJ Int.*, 61:2915–2922.
- Martinsson, J, 2018. A Study of the Behavior of Foaming Slag in Steelmaking, Stockholm, ISBN 978-91-7729-828-1.
- Roscoe, R, 1952. The Viscosity of Suspensions of Rigid Spheres, *Br. J. Appl. Phys.*, 3:267-269.
- Saito, N, Hara, D, Teruya, S, Nakashima, K, 2020. Viscosity of Slag Suspensions with a Polar Liquid Matrix, *ISIJ Int.*, 60:2807-2818.
- Stokes, G G, 1845. On the Theories of the Internal Friction of Fluids in Motion, and of the Equilibrium and Motion of Elastic Solids, *Trans. Camb. Philos. Soc.*, 8:287-319.